Regenerative Therapy 19 (2022) 131–143

Contents lists available at ScienceDirect

Regenerative Therapy

journal homepage: http://www.elsevier.com/locate/reth

Original Article

Repair of ovine peripheral nerve injuries with xenogeneic human acellular sciatic nerves prerecellularized with allogeneic Schwann-like cells—an innovative and promising approach

Florencia-E. Pedroza-Montoya [a], Yadira-A. Tamez-Mata [b], Mario Simental-Mendía [b], Adolfo Soto-Domínguez [c], Mauricio-M. García-Pérez [d], Salvador Said-Fernández [a], Roberto Montes-de-Oca-Luna [c], José-R. González-Flores [d], Herminia-G. Martínez-Rodríguez [a, 1], Félix Vilchez-Cavazos [b, *, 1]

[a] *Autonomous University of Nuevo Leon (UANL), Medicine School, Department of Biochemistry and Molecular Medicine, Av. Madero and Dr. Eduardo Aguirre Pequeño S/N Col. Mitras Centro, Monterrey, Nuevo Leon C.P 64460, Mexico*
[b] *UANL, Medicine School and University Hospital "Dr. José Eleuterio González", Orthopedics and Traumatology Service, Av. Madero and Dr. Eduardo Aguirre Pequeño S/N Col. Mitras Centro, Monterrey, Nuevo Leon C.P 64460, Mexico*
[c] *UANL, Medicine School, Department of Histology, Av. Madero and Dr. Eduardo Aguirre Pequeño S/N Col. Mitras Centro, Monterrey, Nuevo Leon C.P 64460, Mexico*
[d] *UANL, Medicine School and University Hospital "Dr. José. Eleuterio González" Service of Plastic Surgery, Av. Madero and Dr. Eduardo Aguirre Pequeño S/N Col. Mitras Centro, Monterrey, Nuevo Leon C.P 64460, Mexico*

ARTICLE INFO

Article history:
Received 25 August 2021
Received in revised form
11 January 2022
Accepted 27 January 2022

Keywords:
Xenograft
Autograft
Acellular graft
Peripheral nerve injury
Schwann-like cells
Sciatic nerve

ABSTRACT

Introduction: The iatrogenic effects of repairing peripheral nerve injuries (PNIs) with autografts (AGTs) encouraged the present study to involve a new approach consisting of grafting xenogeneic prerecellularized allogeneic cells instead of AGTs.
Methods: We compared sheep's AGT regenerative and functional capacity with decellularized human nerves prerecellularized with allogeneic Schwann-like cell xenografts (onwards called xenografts). Mesenchymal stem cells were isolated from ovine adipose tissue and induced in vitro to differentiate into Schwann-like cells (SLCs). Xenografts were grafted in ovine sciatic nerves. Left sciatic nerves (20 mm) were excised from 10 sheep. Then, five sheep were grafted with 20 mm xenografts, and five were reimplanted with their nerve segment rotated 180° (AGT).
Results: All sheep treated with xenografts or AGT progressively recovered the strength, movement, and coordination of their intervened limb, which was still partial when the study was finished at sixth month postsurgery. At this time, numerous intrafascicular axons were observed in the distal and proximal graft extremes of both xenografts or AGTs, and submaximal nerve electrical conduction was observed. The xenografts and AGT-affected muscles appeared partially stunted.
Conclusions: Xenografts and AGT were equally efficacious in starting PNI repair and justified further studies using longer observation times. The hallmarks from this study are that human xenogeneic acellular scaffolds were recellularized with allogenic SCL and were not rejected by the nonhuman receptors but were also as functional as AGT within a relatively short time postsurgery. Thus, this innovative approach promises to be more practical and accessible than AGT or allogenic allografts and safer than AGT for PNI repair.

* Corresponding author. School of Medicine and University Hospital "Dr. José Eleuterio González", Orthopedics and Traumatology Service, Av. Madero and Dr. Eduardo Aguirre Pequeño S/N Col. Mitras Centro, Monterrey, Nuevo León C.P 64460, Mexico.
E-mail addresses: florencia.estefana@gmail.com (F.-E. Pedroza-Montoya), dra.yadiratamez@gmail.com (Y.-A. Tamez-Mata), mario.simental@gmail.com (M. Simental-Mendía), ibqasoto@yahoo.com.mx (A. Soto-Domínguez), drmauriciogarcia@gmail.com (M.-M. García-Pérez), salvador.said@gmail.com (S. Said-Fernández), rrrmontes@yahoo.com (R. Montes-de-Oca-Luna), jraul81@gmail.com (J.-R. González-Flores), herminiamar@gmail.com (H.-G. Martínez-Rodríguez), jose.vilchezc@uanl.mx, vilchez.hu.orto@gmail.com (F. Vilchez-Cavazos).
Peer review under responsibility of the Japanese Society for Regenerative Medicine.
[1] Authors who mainly contributed to the conception, planning, and execution of the present work.

https://doi.org/10.1016/j.reth.2022.01.009

1. Introduction

Peripheral nerve injuries (PNIs) result in partial or complete disruption of normal nerve physiology. Therefore, PNI represents a health problem causing a socioeconomic burden and a poor quality of life for patients [1]. Then, new treatments for PNI aim to diminish iatrogenic effects and promote axonal regeneration and functional recovery as wholly and promptly as possible. When the length of the nerve gap is lower than 10 mm, the nerve stumps can be sutured end-to-end, yielding satisfactory functional recovery [2]. However, for longer gaps, autograft (AGT) implantation—the gold standard—is recommended [3]. Nevertheless, AGT requires two surgical interventions on the patient and involves sacrificing a healthy donor nerve, resulting in donor-site morbidity [3]. In addition, the use of autologous nerve grafts is limited by donor tissue availability [4].

As an alternative, several nerve scaffolds or conduits for repairing PNI have been proposed and assayed, including cadaveric nerves, whose grafting requires immunotherapy and eventually could be rejected by receptors [5]. Another alternative is grafting polymeric conduits, such as chitosan [6] or collagen type I [7,8]. These polymeric bridges are helpful to treat PNIs longer than 20 mm. Regarding polymeric conduits, Silva et al. [9] concluded from a systematic review that these conduit grafts are more desirable than suture repair and nerve grafting, considering that the functionality recovery rates achieved with conduits are above 80%. Nevertheless, Silva et al. [9] suggest that surgeons carefully consider their choice because synthetic conduits have shown high complication rates.

Another alternative is using cadaveric decellularized nerve scaffolds [10], which offer the following advantages: 1) The probability of rejection is minimal [11,12]. 2) Keep the architecture of the nerve stroma [11,12]. 3) Provide physical-structural support for regenerative cell growth into the new nerve segment and contain neurotrophic factors [13–16].

On the other hand, acellular xenogeneic nerves could be a better option than allografts. As discussed below, acellular xenografts offer the same advantages as allogeneic scaffolds and are more abundant, easier to obtain, and imply less practical and ethical restrictions. Currently, xenografts have been assayed mainly in small laboratory animals. For example, Wang et al. [17] found that the axonal regeneration and the functional recovery of the sciatic nerve PNI of Wistar rats grafted with rabbit acellular sciatic nerve were similar to those of allogenic nerve grafts and slightly inferior to those of AGT.

Zhang et al. [15] repaired a sciatic nerve PNI in Sprague Dawley rats with an intercostal nerve of a York swine recellularized with neural cells derived from adipose tissue mesenchymal stem cells. Although the above are promising results, the expectation of using xenografts in humans to repair PNI is just in the earliest stage of its development. Therefore, the next step should be to experiment with peripheral nerve xenografts from middle-sized animals. Unlike small animal xenografts, peripheral nerves from middle-sized domestic animals, such as ovines or swine, have diameters compatible with human nerves and, therefore, would be appropriate for use in humans. Nevertheless, this option still needs to be extensively investigated. Currently, it is impossible to experiment with peripheral nerve acellular allografts in humans due to ethical restrictions, but it is possible to experiment with acellular human peripheral nerve xenografts in middle animals, as we did in this study.

Schwann cells (SCs) are the other essential element for PNI repair with any graft. Adipose tissue mesenchymal stem cells (AD-MSCs) are often employed in conducting studies concerning regenerative medicine of the peripheral nervous system. Adipose tissue mesenchymal stem cells can differentiate in situ or in vitro into Schwann-like cells (SLCs) [6], promoting PNI regeneration, remodeling, and repair [12,18–20]. Therefore, SLCs were included in this study to prepare human-in-ovine prerecellularized xenografts (onwards xenografts).

The present study aimed to investigate a) whether xenografts could be recellularized with allogeneic ovine SCL; b) whether xenografts could start a repair process of the injured sciatic nerve without rejection; and c) how the regenerative and functional ability of the xenografts was compared with that of AGT after a relatively short postimplant time (six months).

2. Materials and methods

2.1. Ovine and sample size determination

Thirteen female sheep (*Ovis aries*) aged six months, weighing 20–30 kg, and clinically healthy were used. Twelve ewes were randomly assigned into two groups (n = 6) based on a random list (https://www.randomizer.org/). One of the 13 sheep was used for the procurement of adipose tissue as a source of AD-MSCs. Six ewes were treated with an AGT, and the other six received acellular human-in-ovine xenografts prerecellularized with allogeneic ovine SLCs (short name, xenografts). Considerable effort was made to minimize the suffering and pain of the animals while considering the use of a minimum number of animals required to obtain reliable scientific data.

According to previous results with a similar evaluation model, the sample size was determined based on two means difference tests [21]. A $z\alpha$ of 1.96 with a significance level of 95% for two tails and a $z\beta$ of 0.84 with 80% power were used. A sample size of 4 animals per group (n = 4) was determined. Nevertheless, we included two extra animals per group, considering probable losses. In the end, two sheep (one from each group) were excluded from the study due to postsurgical complications, leaving five experimental subjects per group for analysis.

2.2. Procurement of human sciatic nerves

Sciatic nerves were procured from two males and one female aged 40–60 years (median of 55 years), without degenerative or infectious diseases, showing severe traumatic brain injuries as a cause of death. Corpses were kept at 4 °C until nerve procurement. After asepsis, an incision from the iliac spine until the foot through the anteromedial region was made. Next, a dissection per layer was made in the thigh until exposure of the sciatic nerve. Subsequently, the nerves were dissected and placed in phosphate-buffered saline (PBS, 0.01 M pH 7.4; Gibco®/Invitrogen™, Grand Island, NY, USA) plus 50 μg/mL gentamicin and 2.5 μg/mL amphotericin B (Gibco®/Invitrogen™, Grand Island, NY, USA) before cleaning and debriding.

2.3. Preparation of the acellular nerve scaffolds

Immediately after procurement, the nerves were submerged in PBS, kept at 4 °C, and removed from the surrounding tissue. Then, the nerves were cut into segments of 20 mm and decellularized according to the method described by García-Pérez et al. [20]. Briefly, the nerve segments were washed five times in 15 mL sterile distilled water, replacing the water every 2 h. The samples were exposed overnight to 3% Triton X-100 (Sigma–Aldrich, St. Louis, MO, USA) aqueous solution under constant agitation (500 rpm/min). The segments were then submerged for 24 h into 15 mL of 4% sodium deoxycholate (Sigma–Aldrich) aqueous solution. The detergent-based decellularization process was repeated seven times every third day under aseptic conditions at room

temperature. Finally, the nerve scaffolds were washed with 15 mL sterile distilled water and stored in 15 mL PBS at 4 °C until use.

2.4. Morphological analysis of the acellular nerve scaffolds

Five of the acellular nerve sections were randomly selected to perform histological analyses. The samples were fixed with 2.5% glutaraldehyde in 0.1 M pH 7.4 cacodylate buffer (Sigma–Aldrich) at 4 °C for 24 h. Then, the samples were processed by the conventional histological technique until their inclusion in paraffin blocks. Longitudinal tissue sections were stained with hematoxylin-eosin (Sigma–Aldrich) to analyze the presence of residual nuclei or cell debris. Additionally, Masson's trichrome and modified Masson's trichrome staining techniques were employed to analyze the conservation of the extracellular matrix (ECM). Specific lipids of the myelin sheaths, aldehyde groups from complex polysaccharides of the ECM, and axons were evaluated with the Klüver-Barrera, Schiff's periodic acid (PAS), and Marsland-Glees' silver impregnation methods, respectively. The acellular nerve scaffolds were compared with nondecellularized nerves and analyzed by optical microscopy (AC 100–240 V, Omax, Kent, Washington, USA). A morphometric analysis of the tissue-engineered nerve was carried out by densitometry in ImageJ software v.1.51 (US NIH, Bethesda, Maryland, USA, https://imagej.nih.gov/ij/) from microphotographs (A35180U3, Omax). According to a methodology already described [22]. These micrographs were taken from 40 random fields from eight slides at a 400X magnification [22].

2.5. Isolation and characterization of AD-MSCs

Twenty-four hours before adipose tissue procurement, one ewe, randomly chosen, was fasted and sedated with intravenous ketamine 10 mg/kg (Anestek, PiSA, Tlajomulco de Zuñiga, Jal. México) and xylazine 0.5 mg/kg (Procin, PiSA) and anesthetized with endotracheal 2 L/min of 3% isoflurane plus 3% oxygen (Sofloran Vet, PiSA). Subcutaneous adipose tissue (20 cm^3) was procured surgically from the abdominal region.

Immediately after the surgery, the adipose tissue was cut into small pieces, mixed with two volumes of a collagenase solution [0.2% type I collagenase in sterile PBS supplemented with 50 μg/mL gentamicin and 2.5 μg/mL amphotericin B (PBS-GA; Gibco®/Invitrogen™, Grand Island, NY, USA)] and incubated at 37 °C and 300 rpm for 60 min. The dispersed cells were washed five times in PBS-GA and centrifuged at 2800×*g* for 5 min. The pellet was resuspended in 5 mL enriched culture medium [Alpha-MEM plus GlutamaxTM-I medium (Gibco®/Invitrogen™) supplemented with 10% fetal bovine serum (FBS; Gibco®/Invitrogen™) and 50 μg/mL gentamicin and 2.5 μg/mL amphotericin B] and incubated for 48 h at 37 °C in a 5% CO_2 atmosphere in 25 cm^2 culture flasks (Corning®, NY, USA). From these cultures, AD-MSCs were selected through three passages, which were performed as follows: the cells not attached to the substrate were discarded by gently washing the cell monolayer with PBS. On the other hand, the attached cells —forming a monolayer— were detached with 1 mL of 0.25% trypsin–EDTA, (Gibco®/Invitrogen™) incubated at 37 °C in a 5% CO_2 atmosphere for about 10 min. The cell suspension was transferred to a 15 mL conic tube, added with 1 mL of enriched culture medium, centrifuged at 2800×*g* for 10 min, and incubated in culture flasks containing 5 mL fresh enriched medium. The cells not attached were discarded by washing the cell monolayer with PBS. The AD-MSCs were characterized by immunocytochemistry (ICC), as described elsewhere [20]. Briefly, the cells were labeled with primary monoclonal antibodies anti-CD105 (1:25 v/v) and anti-CD90 [(1:100 v/v) (US Biological, Salem, MA, USA)]. $CD105^+$ and $CD90^+$ cells were visualized using a mouse- and rabbit-specific HRP/DAB detection system (Abcam®, Cambridge, UK) following the manufacturer's instructions. Histological sections from sheep brain and spleen were used as positive controls. The percentage of $CD105^+$ and $CD\text{-}90^+$ cells was calculated by counting them in eight random fields from four different slides as described above.

2.6. Differentiation of AD-MSCs into SLCs

We adapted the Jiang et al. method [23] to differentiate ovine AD-MSCs into SLCs. Third passage and 60% confluence AD-MSCs (approximately 1×10^5 cells) were induced to differentiate into SLCs. AD-MSCs were cultured with 5 mL MEM-Alpha plus Glutamax medium supplemented with gentamicin/amphotericin (50 μg/mL and 2.5 μg/mL, respectively; MEM-Alpha-GA and 1.0 mM β-mercaptoethanol (Sigma–Aldrich) for 24 h. The spent MEM-Alpha-GA was changed to MEM-Alpha-GA supplemented with 10% FBS and 0.1 mM trans-retinoic acid (Calbiochem®, Merck KGaa, Darmstadt, Germany) and left for 72 h at 37 °C in a 5% CO_2 atmosphere. The above medium was replaced with MEM-Alpha-GA supplemented with 10% FBS, 5.0 mM forskolin (Calbiochem®), 10 ng/mL recombinant human fibroblast growth factor-b (bFGF; Peprotech, Inc., Rocky Hill, NJ, USA), 10 ng/mL recombinant human platelet-derived growth factor-AA (PDGF-AA; Peprotech, Inc.), and 200 ng/mL recombinant human 1β-heregulin (Peprotech, Inc.). This cell culture was incubated at 37 °C in a 5% CO_2 atmosphere until cell cultures reached 80% confluence (6–8 d). Then, the generated SLCs were identified by immunocytochemistry employing a monoclonal anti-S-100 antibody (1:1500, Agilent Dako Cytomation, Inc. Santa Clara, CA, USA), which identifies peripheral nervous system PNS and central nervous system (CNS) myelin-formed cells. The $S\text{-}100^+$ cells were visualized with the same detection system. A sheep brain was used as the positive control. The percentage of $S\text{-}100^+$ cells was calculated by counting the stained cells in eight random fields from four different slides according to the methodology described above.

2.7. Recellularization of acellular nerve scaffold

As a first stage, the acellular nerve scaffolds were immersed once in 15 mL of 70% ethanol (reactive grade, JT Baker, Waltham, MA, USA) for approximately 3.0 s and twice in PBS-GA for 10 s. Then, SLCs (3×10^5 cells) [20] were suspended in 50 μL MEM-alpha-GA culture medium. The cell suspension was carefully spread into and along the acellular nerve scaffold by injecting it with an insulin syringe. For histological analysis, 2 cm sections of prerecellularized scaffolds, nerve submitted to decellularization, and a non-treated nerve section were incubated for 48 h at 37 °C in a 5% CO_2 atmosphere. Then, histological sections from the above preparations were stained with hematoxylin-eosin, observed with a brightfield microscope at 400X magnification, and determined the number of cells in eight fields (each sizing 64 mm^2) from each histological preparation.

The number of SLCs per field was verified on histological sections stained with hematoxylin and eosin in randomly selected acellular/prerecellularized nerve scaffolds.

Six months after grafting, the second stage was performed, consisting of the surgically recovering graphs and involved muscles and evaluating the sheep neurophysiological condition, nerve regeneration, muscular atrophy, and morphological analysis of the tissue-engineered tissue nerves.

2.8. Surgical procedure

All surgeries were performed under aseptic conditions. The sheep were sedated and anesthetized, and then a 90 mm incision

was made in the lateral gluteal region of the left posterior limb to expose the sciatic nerve. Then, a 20 mm sciatic nerve segment was excised in the AGT group, turned 180°, and sutured in the gap left by the same nerve segment. On the other hand, a 20 mm segment of the sciatic nerve was surgically excised in the xenograft group, and the gap was filled with a xenograft. Next, the proximal and distal extremes of xenografts or AGTs were sutured with 9/0-gauge nylon sutures (Atramat®, Mexico City, Mexico). Then, the surgical wound was fastened by plans with 3-0 resorbable polyglactin sutures (Vicryl, Ethicon, Somerville, NY, USA). Fig. 1 shows the main surgical steps of nerve gap creation and grafting.

After the surgery, the sheep were closely monitored during their anesthetic recovery and injected with 1 mL/10 kg intramuscular clindamycin and gentamycin (Clindagen, Mederilab, Jalisco México). In addition, 1 mL/40 kg meglumine of flunixin (Megludol, Medderilab, Mexico City, Mexico) was administered every 24 h for three days for pain management. During the entire postsurgical observation period, the animals had water and food ad libitum. Mobility recovery of each sheep intervened limb, and the hind limbs' gait and coordination were documented once a month for six months. A PVC splint designed for each sheep was held with a bandage to prevent the operated limb from further injuries during the recovery period.

2.9. Neurophysiologic evaluation

Six months after surgery, the electrophysiology of the grafted nerves and the involved muscles were evaluated. The sheep were left fasted for 24 h and then sedated and anesthetized. The sciatic nerve was exposed, and the nerve trunk was stimulated 5 mm upward (preinjury), proximal anastomosis and 5 mm downward (postinjury) distal anastomosis. The contralateral sciatic nerves from both the AGT and xenograft groups were exposed to electrophysiology and analyzed as nonintervening contralateral limb controls (NICs). The exposed nerves were stimulated by applying a supramaximal electrical potential (34 V), and the electromyographic response of the biceps femoris and gastrocnemius, including amplitude, latency, and conduction velocity, was recorded with a Nicolet Viking electrodiagnostic system (Nicolet Instrument Corporation, Madison, WI, USA).

The amplitude (reported mV) is defined as the maximum variation from the negative peak regarding the baseline. The latency is defined as the time (reported in ms) elapsed between the application of the electrical stimulus and the observation of electrical response. The nerve conduction velocity was calculated as the distance between the electrodes and the time for electrical impulses to travel between the preinjury and postinjury locations (21 cm) divided by the preinjury minus the postinjury latency. These parameters were recorded and evaluated in a blinded manner in both the AGT and xenografts compared with their corresponding contralateral nonintervened sciatic nerves.

2.10. Evaluation of nerve regeneration and muscular atrophy

After the neurophysiological evaluation, all sheep were euthanized with an intravenous overdose of sodium pentobarbital (90–210 mg/kg; Pisabental, PiSA). The biceps femoris and gastrocnemius muscles from both limbs were excised. The total extension of AGT or xenografts plus 10 mm of nonintervened nerve placed in both proximal and distal extremes of grafts and 40 mm from the contralateral sciatic nerve were also excised. The muscles were analyzed macroscopically and weighed. Atrophy of the biceps femoris and gastrocnemius, along with the wet weight ratio, were determined using the following equation: wet weight ratio = wet weight on the operated limb/wet weight of the contralateral limb × 100 [24].

2.11. Morphological analysis of the nerve regeneration

The excised grafts were processed to evaluate the axonal regeneration, recellularization, and integrity of the ECM following the above-described immunohistochemical and histochemical methods. Additionally, the presence of SLC (S-100$^+$) and neurofilaments in axons (NF$^+$) was examined through immunohistochemistry in the study groups. The contralateral nonintervened sciatic nerve segments (NICs) were used as controls. Each of the histological techniques was performed and analyzed in the proximal and distal regions from each sample. The analytical procedure was performed as done with the above-described morphological analysis of the acellular nerve scaffolds.

2.12. Statistical analysis

The normal distribution of all data included in this study was estimated using the Kolmogorov–Smirnov test. A t-test was used to compare results showing a normal distribution between groups of morphometric analyses of the acellular nerve grafts and wet muscle weight data for independent samples. For nonnormal distributions, the Mann–Whitney U test was used. The data of the neurophysiological tests were analyzed employing one-way

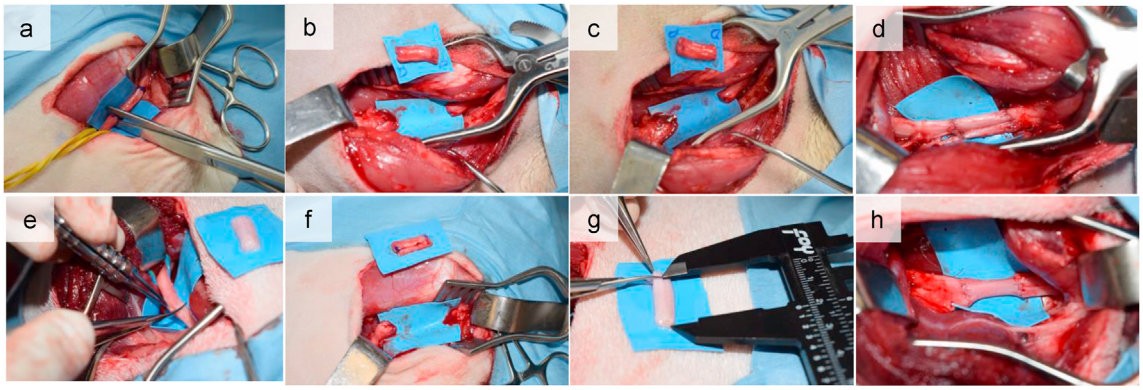

Fig. 1. Surgical steps practiced with the sciatic nerves. Frame a) Sciatic nerve identification and creation of a nerve gap for autograft (AGT). b) Obtention of the AGT. c) AGT rotation (180°) and implantation. d) AGT neurorrhaphy in the sciatic nerve. e) Sciatic nerve identification and creation of a nerve gap for grafting with Schwann-like cell-prerecellularized humans in ovine xenografts (short name, xenografts). f) Creation of nerve gap for xenografts grafting. g) xenografts ready for the implant. h) xenografts neurorrhaphy in the sciatic nerve.

analysis of variance (ANOVA) and the Scheffé post hoc test for multiple comparisons since all the analyzed variables had a normal distribution but a different sample number. ANOVA and Scheffé post hoc tests for multiple comparisons were applied for the morphological evaluation of nerve regeneration data if they had a normal distribution. The Kruskal–Wallis and post hoc Mann–Whitney U tests under Bonferroni tests were used for data with nonnormal distribution. In all data, $p < 0.05$ was considered statistically significant. Data are reported as the mean ± standard deviation (SD). All statistical analyses were carried out using SPSS version 20 (SPSS, Armonk, NY, USA) and GraphPad Prism® (San Diego, CA, USA) software for Macintosh.

2.13. Ethical considerations

Authorized this study, the Research Committee, the Research Ethics Committee, and the Committee for the Care and Use of Laboratory Animals of the Medicine School and University Hospital Dr. José Eleuterio González, under registration #OR17-00001. The sheep used as experimental models were managed following the current International Standards (UK Animal Scientific Procedures Act, 1986 and associated guidelines), the European Communities Council Directive of 24 November 1986 (86/609/EEC), The National Institutes of Health guide for the care and use of laboratory animals (NIH Publications No. 8023, revised 1978), and the Official Mexican Standards for the handling of experimental animals (NOM-062-ZOO-1999). Furthermore, all procedures in procuring the human nerve samples were performed according to the Regulation of the general health law in matter of sanitary control of the disposal of organs, tissues and corpses of human beings (*Reglamento de la ley general de salud en materia de control sanitario de la disposición de órganos, tejidos y cadáveres de seres humanos*).

3. Results

3.1. Morphological and densitometric analysis of the acellular nerve scaffold

Fig. 2a shows a typical image of a decellularized nerve scaffold consisting of the absence of nuclei or cell debris, minimal myelin content and low axonal integrity, complex polysaccharides located in the ECM, normal ECM structural organization, and continuity of collagen fibers. Unlike the healthy control nerve (664 ± 203 cells), cells in the decellularized nerve scaffold were absent (Fig. 2b). The acellular nerve had 3.5 times fewer myelin density units [DU]) ($3.97 \times 10^8 \pm 1.29 \times 10^8$ DU; $p < 0.001$) than NIC's ($1.13 \times 10^9 \pm 3.29 \times 10^8$) and the difference between the axonal positivity ($2.62 \times 10^8 \pm 1.40 \times 10^8$ DU) was 4.4 times lower than the NIC ($1.14 \times 10^9 \pm 1.87 \times 10^8$ DU); $p < 0.001$) (Fig. 2c). No significant differences in the presence of collagen fibers and the complex polysaccharides of the ECM (components of the ECM) were detected for decellularized and control nerves.

3.2. Predifferentiation of AD-MSCs into SLCs

Fig. 3 shows panoramic (b) and close-up (c) images of AD-MSC $CD90^+$, AD-MSC $CD105^+$ (e), panoramic (f), and close-up images before induction to differentiate into SLCs. After AD-MSCs were induced to differentiate into SLCs, these cells became $S100^+$ (Frame h shows a panoramic image and i and close-up showing the S100

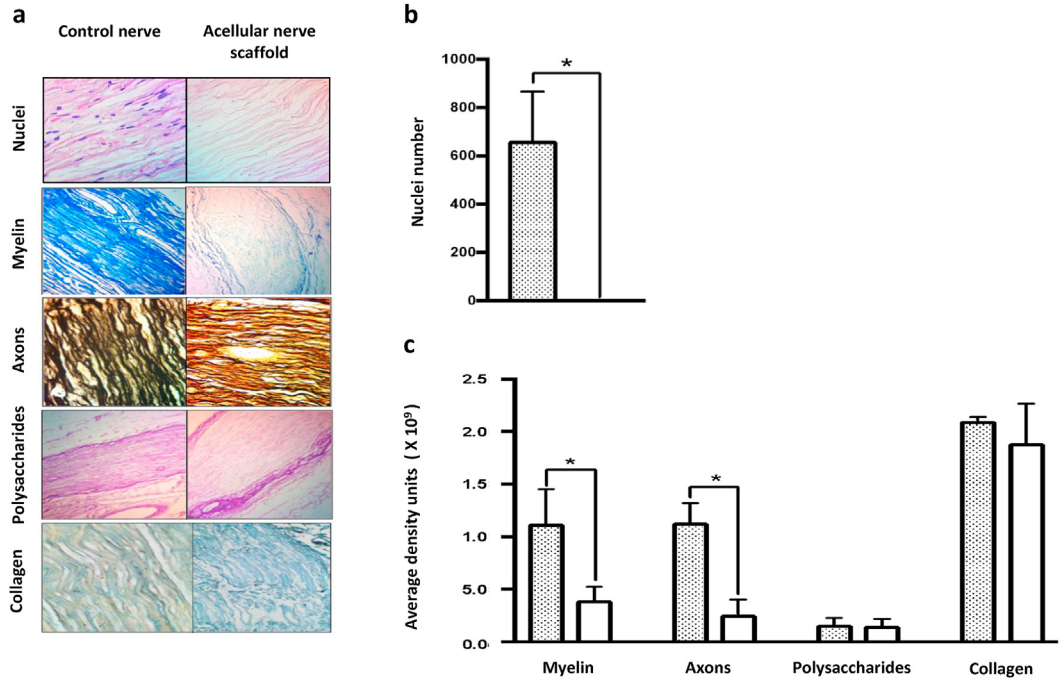

Fig. 2. Morphological and densitometric analysis of the human acellular nerve scaffold performed after the decellularization process. a) Microphotographs from longitudinal sections of a human control nerve (left column) and an acellular human nerve scaffold (right column). Histological sections of the nerve scaffolds were viewed under a brightfield microscope after different staining procedures. Typical photograms represent the following staining techniques and morphological or densitometric analyses. From top to bottom (image amplification is expressed as X): a) Hematoxylin-eosin, showing the presence of cells (dark points) in the control nerve and their absence in the acellular nerve scaffold (400X). Klüver-Barrera, showing myelin lipids in control and decellularized sheath nerves, respectively (100X). Silver impregnation of Marsland-Glees showing axons in both control and decellularized nerves (400X). Schiff's periodic acid, complex polysaccharides' aldehyde groups of the extracellular matrix (ECM [100X]). Modified Masson's trichrome staining showing the ECM (100X). b) Analysis of the number of cells observed in control and decellularized nerves. c) Densitometric analysis of myelin contents, axons, polysaccharides, and collagen determined in histological sections of a control nerve and an acellular nerve scaffold. The densitometry of microphotographs was taken at 400X magnification from 40 random fields taken from eight slides. Data are presented as the mean ± SD ($n = 12$ fields/group for each technique). The asterisk indicates a significant difference between values of both bars ($*p < 0.05$) using the Mann–Whitney U test to compare differences between the variables (cells, myelin, and axons) and t-test for independent samples for polysaccharides and collagen.

marker on their surface. In addition, as positive controls, CD90^{+} (a) and CD105^{+} (d) cells were observed in histological sections from ovine spleen endothelium, and CD100^{+} neurons were observed in ovine brain sections. Frame g is a typical image of S100^{+} cells in an ovine brain section. Frames h and i show S 100^{+} cells, corresponding to AD-MSCs induced to differentiate into SLCs being S100^{+}. Panel j shows that most cells from adipose tissue culture showed markers of MSCs, 88.4 CD90+ and 77.3% CD105^{+}. On the other hand, after induction, most of these cells (66.6%) showed S100^{+} on their surface, the SCLs marker. The remaining AD-MSCs stayed undifferentiated when these were inoculated into de acellular nerve scaffolds.

3.3. Recellularization of the acellular nerve scaffold with SLCs

Fig. 4 shows the appearance of histological sections of a nerve scaffold submitted to a decellularization procedure, an acellular scaffold prerecellularized with SLCs, and a nontreated nerve section, after being incubated for 48 h at 36 °C in a 5% CO_2 atmosphere. The frames A to C show different concentrations of well-conserved

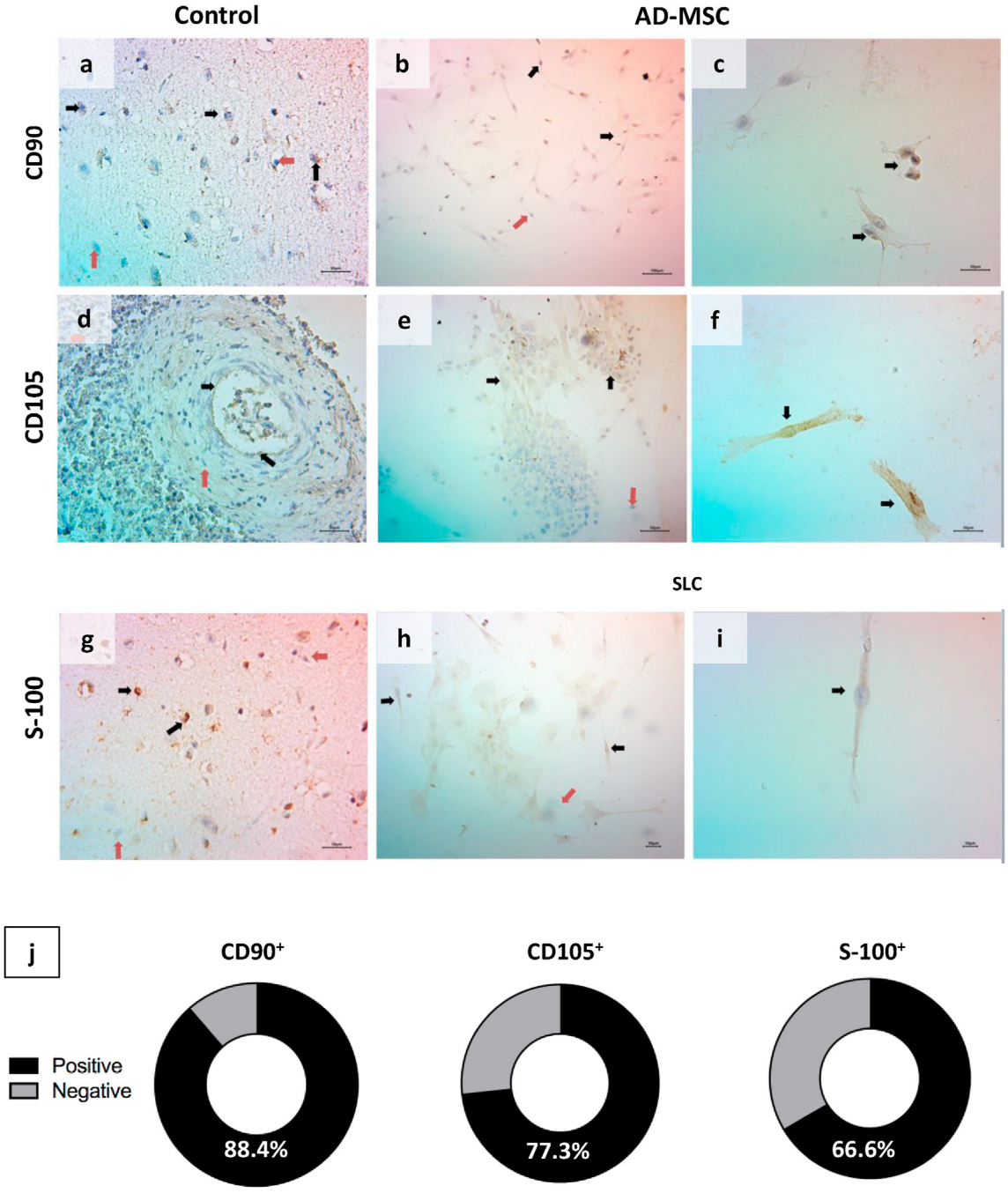

Fig. 3. Labeling of adipose tissue-mesenchymal stem cells (AD-MSCs) and Schwann-like cells (SLCs) by immunohistochemistry. Frames are typical images observed with a light microscope. The arrows signal cells positively (black) or negatively (red) labeled with the monoclonal antibodies named in the left margin. The left column corresponds to controls: a) and d) ovine spleen endothelium and g) ovine brain. The left and central columns correspond to images observed at 100X and the right column at 400X. Panel j) shows the percentages of AD-MSC CD90^{+} and CD105^{+} cells before being induced to differentiate into SCLs and the percentage of S100^{+} cells after the induction procedure.

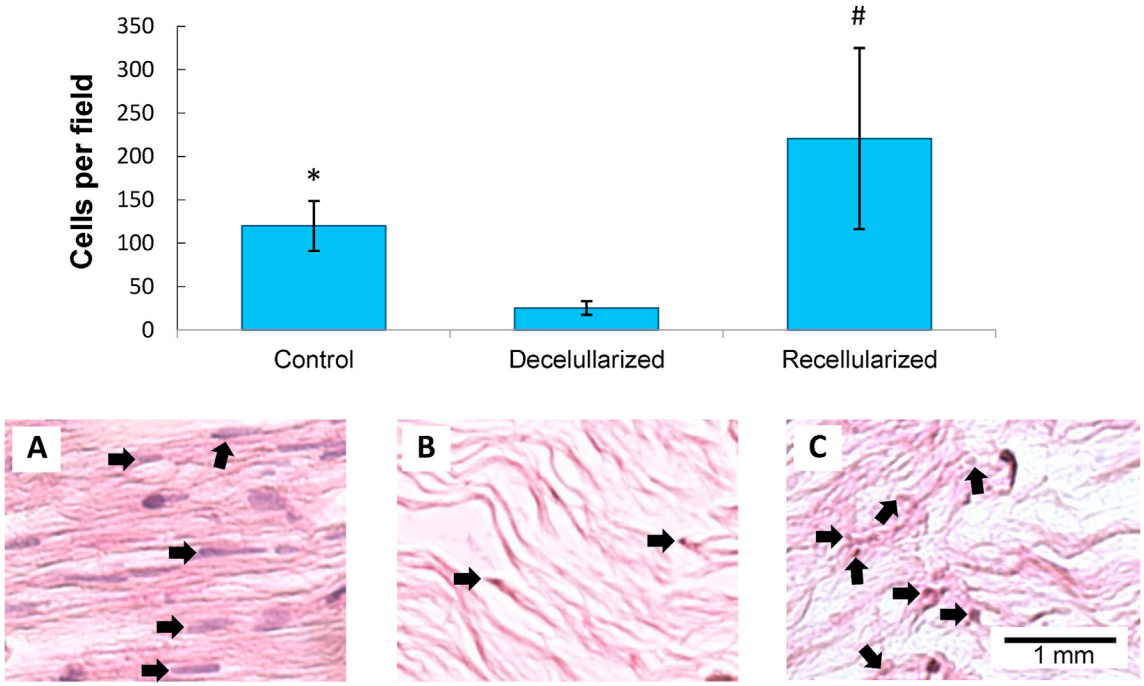

Fig. 4. Prerecellularization of human nerve scaffold with Schwann-like cells (SLCs). Samples (2 cm long) of the nontreated sciatic nerve (frame A), human nerve submitted to a decellularization procedure (frame B), and acellular human scaffold prerecellularized with SLCs (frame C) were incubated at 37 °C in a 5% CO_2 atmosphere for 48 h. Then, the histological sections were stained with hematoxylin-eosin, observed with a brightfield microscope at 400X magnification, and determined the number of cells in eight fields (each sizing 64 mm^2). The columns represent the mean ± SD of eight determinations (n = 8). A t-test for independent samples was used to determine significant differences (*p < 0.05; #p < 0.001) between samples. Arrows indicate the presence of cells.

Fig. 5. Evolution of the sheep grafted limbs. The images illustrate the improved strength and functionality of the sheep legs implanted with autografts (AGT) or human-in-ovine prerecellularized with Schwann-like cell xenografts (short name, xenografts) six months after surgery. During this lapse, the sheep's intervened limbs went from being dragged to present a point of support.

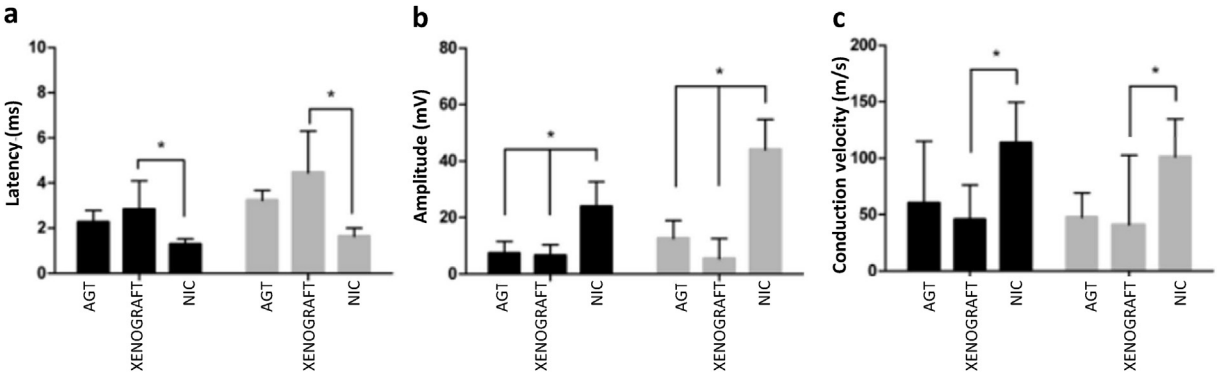

Fig. 6. Neurophysiological evaluation. Six months postsurgery, the exposed nerves from the grafted and nonintervened contralateral nerves were stimulated by applying a supramaximal electrical potential (34 V), and the electromyographic response of the biceps femoris and gastrocnemius was recorded with a Nicolet Viking electrodiagnostic system. The graph shows the neurophysiological values of the biceps femoris and gastrocnemius at six months postgrafting. The acronyms indicate autograft (AGT); human-in-ovine prerecellularized with allogeneic ovine Schwann-like cells (xenografts), nonintervened contralateral limb (NIC). Data are presented as the mean ± SD (n = 5 for AGT and xenografts; n = 10 for NIC). One-way analysis of variance (ANOVA) was used to determine significant differences (*p < 0.05) between the means of the variables. Scheffé's post hoc analysis was used to confirm the differences between AGT and xenograft groups, and each of these and NIC.

cells. Resident cells from the nontreated nerve appear larger than SLCs and fully extended, and SLCs appear less extended due to the short incubation elapsed time since their inoculation. Quantitative analysis revealed that the nerves submitted to a decellularization procedure contained 25.5 ± 7.9 cells/field, the nontreated nerve 119.9 ± 28.8 cells/field, and the prerecellularized nerve scaffold 220.6 ± 104.1 cells/field. That is to say, the prerecellularized nerve scaffold contained 8.7 times more cells per field than the acellular scaffold and 1.8 more cells than the non-treated nerve. Differences between the prerecellularized nerve and the scaffold submitted to decellularization and between the nontreated nerve and the prerecellularized nerve were significant ($p < 0.0001$ and $p < 0.05$, respectively).

3.4. Postsurgical inspection

During the first two months of the postsurgical period, no significant changes were observed in the mobility of the intervened limb in the AGT or xenograft sheep groups. Between the third and fourth months postsurgery, the mobility in all sheep's tibia and fibula regions was improved. Nevertheless, all ewes presented lameness and difficulty walking, manifested by an abnormality in the plantar flexion of the metatarsophalangeal joint. During the fifth and sixth months, all sheep from both the AGT and xenograft groups showed a slight improvement in metatarsus mobility and strength. Three of the five sheep from AGT and xenografts went from being dragged postsurgery to presenting foothold during the march at six months, although claudication was still observed (Fig. 5).

3.5. Neurophysiological evaluation

Fig. 6 shows the results of the biceps femoris and gastrocnemius electromyographic response. Latency in the biceps femoris (Fig. 6a) was significantly higher in the xenograft (2.84 ± 1.27 ms) than in the NIC biceps femoris (1.28 ± 0.25 ms; $p = 0.003$). No significant differences were observed between the AGT and NIC or between the AGT and xenograft sheep groups. The gastrocnemius latency (Fig. 6a) of xenografts (4.34 ± 1.76 ms) was significantly higher than that of the NIC gastrocnemius (1.88 ± 0.34 ms; $p = 0.001$). No significant differences were observed between AGT and the NIC or the AGT and the xenograft group.

The amplitude of the electromyography response (Fig. 6b) in both the AGT (7.30 ± 4.16 mV) and the xenograft biceps femoris (6.60 ± 3.75 mV) was significantly lower than that of the NIC (23.89 ± 11.54 mV; $p < 0.00001$). No significant differences were observed between the AGT and xenograft groups. Similarly, the amplitude recorded for the gastrocnemius in the AGT (12.60 ± 6.36 mV) and xenograft (5.18 ± 7.35 mV) groups was significantly less than that of their NIC (44.11 ± 11.89 mV; $p < 0.00001$). No significant differences were found in the amplitude of the electromyography response of the gastrocnemius between the AGT and xenograft groups.

A higher conduction velocity was detected in the NICs for both the biceps femoris and the gastrocnemius compared with their respective AGT or xenograft interventions (Fig. 6c). However, in the biceps femoris, the conduction velocity of xenografts (45.80 ± 30.48 m/s) was significantly lower than that of NICs (113.50 ± 34.00 m/s; $p = 0.02$). In addition, the conduction velocity in the gastrocnemius was significantly lower in the xenograft group

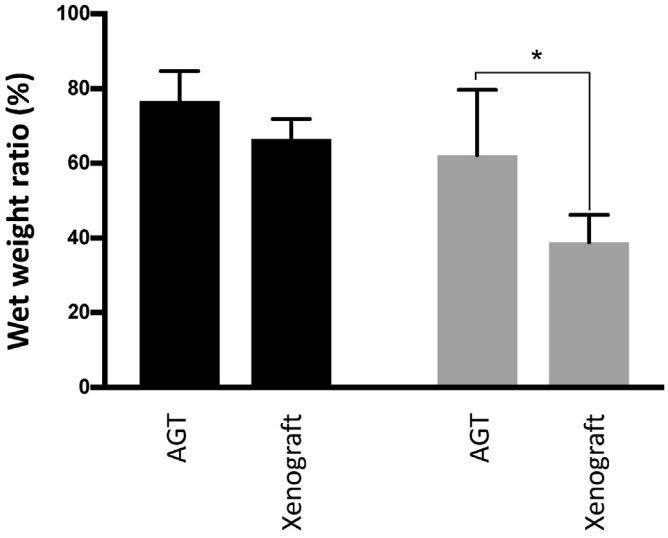

Fig. 7. Evaluation of muscular atrophy. Acronyms are AGTs, autografts, xenografts, and human-in-ovine xenografts prerecellularized with allogeneic ovine Schwann-like cells. Black and gray columns correspond to biceps femoris and gastrocnemius measures, respectively. The 100% wet weight ratio corresponds to the control muscles of the contralateral limb. Each column corresponds to the mean ± SD of measures from five (n = 5) intervened limbs with AGT or xenografts. A t-test for independent samples was used to determine significant differences (*p < 0.05) between AGT and xenografts.

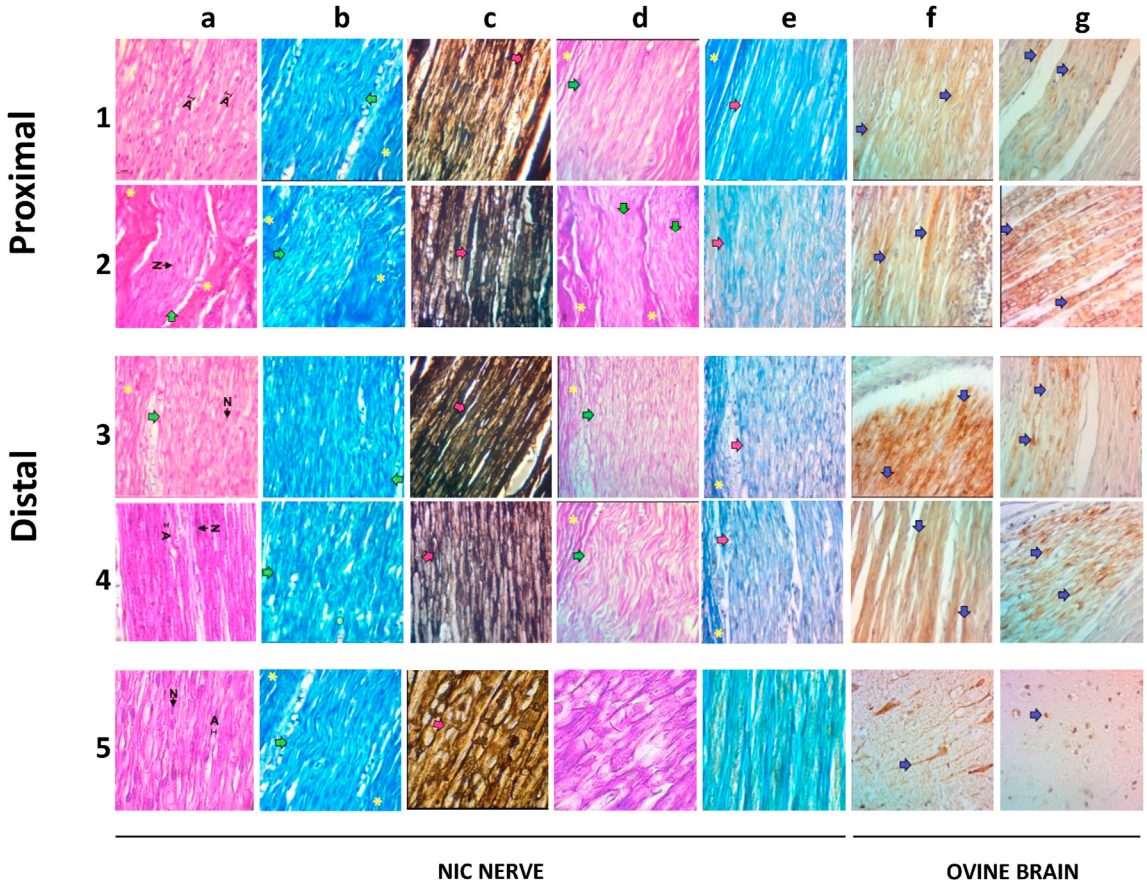

Fig. 8. Morphological analysis of organized regions of autografts (AGT) and human-in-ovine xenografts prerecellularized with Schwann-like cells (short name, xenografts). The images correspond to typical histological sections of nerve implants observed with a brightfield microscope at 400X magnification. Rows 1 and 2 correspond to proximal implant sections: Row 1 to an autograft (AGT) and row 2 to a xenograft. Rows 3 and 4 show images from the distal sections of AGT and xenografts, respectively, row 5 of controls. Frames 5a to 5e correspond to histological sections from nonintervened contralateral nerves (NICs), and 5f and 5g are section images from ovine brains. The staining methods mentioned below were used to visualize the following graft structures: a) hematoxylin-eosin, cells; b) Klüver-Barrera, myelin sheath; c) Marsland-Glees silver impregnation, axons; d) Schiff's periodic acid, extracellular matrix (ECM) polysaccharides; e) modified Masson's trichrome, ECM collagen. Using immunocytochemistry methods, frame f) shows neurofilaments (NF) labeled with monoclonal anti-NF, and g) Schwann-like cells visualized with anti-S-100. Symbols inside the photograms signal connective tissue (*); axons (A); green arrows, cells; red arrows, axon fascicles; blue arrows, axonal disruptions.

(41.00 ± 61.70 m/s) than in the NIC group (101.30 ± 32.41 m/s; $p = 0.041$). No significant differences were recorded between the AGT and xenograft groups.

3.6. Evaluation of the muscular atrophy

Fig. 7 shows no significant differences in the wet weight ratio from the biceps femoris between AGT (76.73% ± 7.98%) and xenografts (66.52% ± 5.36%). On the other hand, the wet weight ratio of the gastrocnemius from xenografts (38.88% ± 7.32%) was significantly lower than that of AGT (62.24% ± 17.43%; $p = 0.039$).

3.7. Graft morphologic evaluation

3.7.1. Recellularization and nerve architecture in graft-organized regions

Fig. 8 shows that the proximal and distal regions of AGT and xenografts contained organized areas of connective tissue, fascicles of axons, and cell distribution. The organized areas were composed of individualized fascicles of axons with parallel orientation and variable diameter. In addition, myelin sheaths with their characteristic zigzag pattern and elongated cell nuclei from SLCs and fibroblasts can be observed, all wrapped by connective tissue (Fig. 8 a1-a4). This fascicle arrangement and cell population in the AGT and xenograft groups were similar to those of NIC nerves (Fig. 8 a5).

3.7.2. Remyelination

Fig. 8 b5 shows myelin surrounding the axons in fascicular structures in the NIC nerve. This pattern was also observed in the organized areas of the AGT and xenografts (Fig. 8b) (b1-b4). Interestingly, remyelination was observed in the proximal and distal regions of the AGT and xenografts, contrasting with the significant lack of myelin in the acellular scaffold (Fig. 2a).

3.7.3. Axonal nerve architecture

Throughout, AGT and xenografts contain organized and continuous fascicles with intrafascicular axons having homogeneous calibers (Fig. 8 c1-c4). These patterns are similar to NIC's (Fig. 8 c5).

3.7.4. Integrity of the ECM

Fig. 8 d1-d4 shows the ECM, which presents a typical structure surrounding the nerve fibers forming fascicles in the organized regions of AGT and xenografts. These structures are similar to those presented by NIC nerves (Fig. 8 d5). On the other hand, collagen fibers were observed as continuous and organized blue lines in AGT and xenografts (Fig. 8 e1-e4), corresponding to the typical structure

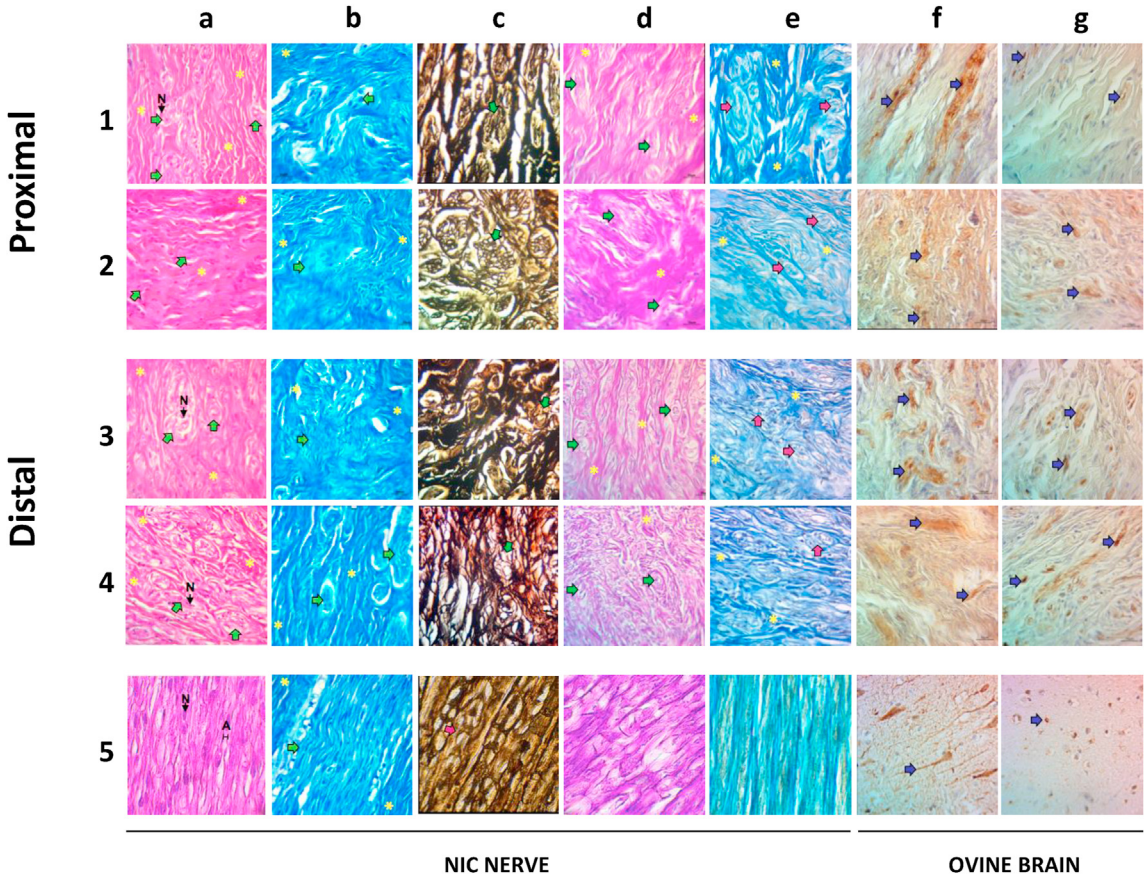

Fig. 9. Morphological analysis of disorganized regions of autografts (AGT) and human-in-ovine xenografts prerecellularized with Schwann-like cells (xenografts). The images correspond to typical histological sections of nerve implants observed with a brightfield microscope at 400X magnification. Rows 1 and 2 correspond to proximal implant sections: Row 1 to an autograft (AGT) and row 2 to a xenograft. Rows 3 and 4 show images from the distal sections of an AGT and a xenograft, respectively, row 5 of controls. Frames 5a to 5e correspond to histological sections from nonintervened contralateral nerves (NICs), and 5f and 5g are section images from ovine brains. The staining methods mentioned below were used to visualize the following graft structures: a) hematoxylin-eosin, cells; b) Klüver-Barrera, myelin sheath; c) Marsland-Glees silver impregnation, axons; d) Schiff's periodic acid, extracellular matrix (ECM) polysaccharides; e) modified Masson's trichrome, ECM collagen. Using immunocytochemistry methods, frame f) shows neurofilaments (NF) labeled with monoclonal anti-NF, and g) Schwann-like cells visualized with anti-S-100. Symbols inside the photograms signal connective tissue (*); axons (A); green arrows, cells; red arrows, axon fascicles; blue arrows, axonal disruptions.

of the ECM in the NIC nerve (Fig. 8 e5). The arrangements of the fibers show typical structures of the collagen fibers.

3.7.5. *Myelin neurofilaments and SLC immunolabeling in AGT and xenografts*

Fig. 8 f1-f4 shows myelin^{+} neurofilaments in the proximal and distal regions of both AGT and xenografts, demonstrating the presence of axons in both groups. S-100^{+} cells (Fig. 8 g1-g8) were also observed in the proximal and distal regions of both AGTs and xenografts (Fig. 8 g1-g4). Myelin^{+} neurofilaments and S100^{+}, expressed by SCs, were observed in ovine brain sections used as internal controls (Fig. 8 f5 and g5, respectively).

3.7.6. *Recellularization and nerve architecture in graft-disorganized regions*

Fig. 9 shows that both AGTs and xenografts have distal and proximal unorganized regions. Fig. 9 a1-a4 shows an anarchic arrangement of connective tissue fibers. In the middle of these disorganized areas, dense material was apparent, containing small fascicles and a lack of parallel orientation. Myelin is observed in small fascicles (Fig. 9 b1-b4).

Fig. 9 c1-c4 shows many extrafascicular axons mixed with connective tissue, lacking continuity and caliber uniformity, unlike NIC nerves (Fig. 9 c5).

In Fig. 9 d1-d4 ECM is observed surrounding small, disorganized fascicles. In addition, the ECM does not show a linear pattern in the fascicles. Collagen fibers were more abundant in the disorganized regions than in the graft-organized areas (Fig. 9 e1-e4). All the above findings contrast with the organized regions of NIC nerves (Fig. 9 e5).

Fig. 9 f1-f4 shows jumbled neurofilaments and SLCs (Fig. g1-g4) in AGT and xenograft proximal and distal regions. An ovine brain section used as an internal control for myelin and SC was included (Fig. 9 f5 and g5, respectively).

3.7.7. *Densitometric evaluation of nerve regeneration*

Fig. 10 shows significantly higher myelin deposition in the distal regions of the AGT ($2.05 \times 10^{9} \pm 4.71 \times 10^{8}$ DU) than in the NIC ($1.34 \times 10^{9} \pm 1.61 \times 10^{8}$ DU; $p = 001$) and the proximal regions of xenografts ($1.72 \times 10^{9} \pm 3.81 \times 10^{8}$ DU), $p = 0.013$. On the other hand, no significant differences were observed in axon density from distal and proximal regions between AGT and xenografts.

A significantly higher presence of collagen fibers was detected in the proximal region of AGT ($1.61 \times 10^{9} \pm 4.16 \times 10^{8}$ DU) than in the proximal region of xenografts ($1.23 \times 10^{9} \pm 3.68 \times 10^{8}$ DU; $p = 0.034$). On the other hand, no significant differences were observed in the optical density of polysaccharides or collagen fibers between the distal regions of AGT, xenografts, and NICs.

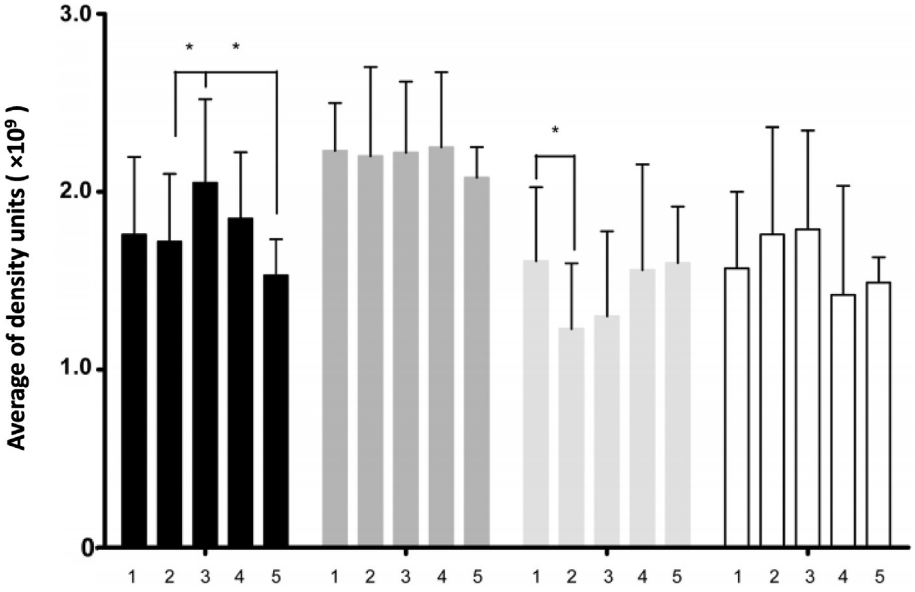

Fig. 10. Graft densitometric analysis. Histological sections from nerve grafts and nonintervening contralateral nerves (NICs) recovered at six months postsurgery were stained and analyzed by optical microscopy, and the optical densities of myelin (black columns), axons (heavy gray), collagen (light gray), and polysaccharides (white) were measured with ImageJ software v.1.51. Numbers in the graphic bottom indicate densitometry columns of 1) proximal autografts (AGT), 2) proximal human-in-ovine xenografts prerecellularized with Schwann-like cells (short name, xenografts), 3) Distal AGT, 4) distal xenograft, 5) NIC. Data are presented as the mean ± SD from 8 random microphotograph fields at 400X magnification per each of the 5 study animals (n = 40). One-way analysis of variance (ANOVA) with Scheffé's post hoc analysis and Kruskal–Wallis with Bonferroni post hoc tests were used to determine significant differences (*p < 0.05) between variables.

4. Discussion

New and better procedures to repair PNI are needed, avoiding sacrificing functional and healthy peripheral nerves, which are currently used to perform autografts. Cadaveric acellular nerve allografts recellularized with autologous SCs or SLCs are considered a good alternative for AGT, mainly because acellular nerves promote PNI and are minimally immunogenic [25,26]. Nevertheless, the procurement of cadaveric material is subject to legal, ethical, and practical restrictions [27–29]. In addition, getting enough quantity of SC or SLCs takes a long time (from 4 to 15 weeks, respectively) [20,30], and the lapse transcurred between a PNI accident and the SC, or SLCs transplantation is crucial [31]. Therefore, a better option could be used acellular xenografts recellularized with allogeneic SLCs, because this material could be pre-produced and stored, being ready when needed. This study is the first step done in this direction.

We previously showed the efficacy of allogeneic (mice) recellularized acellular nerve scaffolds precellularized with allogeneic (mice) SLCs [20]. Now we took advantage of this experience to upward our aims to a middle-sized animal model (sheep) and using xenogeneic- instead of allogenic-grafts and kept using allogeneic (sheep) SLCs to recellularize the nerve scaffold.

During the observation period, the sheep from the xenograft and AGT groups showed a gradual improvement in their grafted leg functionality and strength. However, when the study finished, at sixth month postsurgery, the physical improvement was not total, and the biceps femoris and gastrocnemius muscles appeared partially atrophied. Then, the grafted nerves and the affected muscles of the xenograft and AGT groups could still undergo regenerative processes, as observed in other studies. For example, Forden et al. [32] analyzed the PNI repair process at six and nine months postsurgery in six sheep autografted with a segment of the radial sensory nerve onto a gap created in the median nerve. They noted that both conduction velocity and amplitude increased with time after surgery but did not attain typical values within the observation period. Lawson et al. [33] and Casañas et al. [34] reported progressive but incomplete regeneration of grafted nerves and muscles after their respective observation periods. Gersey et al. [35] published that they treated two human subjects with AGTs enriched with cultivated autologous SC. One patient was followed for 12 months and another for 36 months. After their respective observation periods, both patients had significant—but not total—improvement in motor and sensory functions.

The presence of disorganized areas containing extrafascicular axons observed in both AGTs and xenografts has been observed in many nerves in the process of repair, either into grafts or end-to-end nerve repair. For example, Graham et al. [36] reported that 28 weeks after rat sciatic nerve transection was repaired end-to-end, the nerve presented well- and disorganized areas with extrafascicular axons. Forden [32], after nine months of AGT in the median nerve of sheep, found more extrafascicular connective tissue in the grafted nerves than in controls and some extrafascicular axons. Moore et al. [37] compared the effects of cold-preserved, detergent-processed, and processed acellular nerve allografts with nerve isografts and silicone nerve guidance conduits in a 14-mm rat sciatic nerve gap. After six weeks of grafting, electron micrographs showed viable nerve fibers displaying normal myelination patterns in nerve segments distal to all implanted nerve grafts. Nevertheless, numerous unmyelinated axons were also observed in interposed nerve grafts. Nerve tissue obtained distal to implanted silicone nerve guidance conduits did not reveal any viable myelinated or unmyelinated axons. Additionally, nerve tissue distal to interposed conduits demonstrated numerous signs of progressive Wallerian degeneration and disorganization of the extracellular matrix.

Regarding the graft size, long (>20 mm) or very long (up to 70 mm) autologous or allogeneic xenografts have been used in experimental animals [15,17] or humans [38]. However, experience with xenografts is very scarce, and it has been achieved mainly

from experiments performed in small laboratory animals. In most of these studies, satisfactory results have been obtained using 10 mm grafts [17,39]. Furthermore, Pover et al. [40] did not find significant differences in regeneration success through 10, 20, and 30 mm autografts in cats. Since a few years ago, some clinical experience in humans has been achieved with decellularized peripheral nerve grafts. For example, Karabekmez et al. [41] reported good results using 20 mm on average decellularized nerve allografts to repair sensory defects in the hand. Therefore, considering the lack of experience with xenogeneic grafts in middle animals—nearer to humans than small animals—we took advantage of the experience with allogeneic grafts to take a step that was still unexplored, using 20 mm xenogeneic grafts. Moreover, considering the results shown here and the experience of Pover et al. [40], there seems to be no difficulty in experimenting with longer xenografts and times.

We propose developing a procedure for using xenogeneic acellular peripheral nerves prerecellularized with allogeneic SCL because, unlike cadaveric allografts, nerves of any required diameter and length could be procured from middle-sized domestic animals, such as sheep, swine, or goats, in an unlimited manner and without significant ethical restrictions. Nerves could be procured, decellularized, appropriately prepared, and stored until use. On the other hand, MSCs could be procured from healthy volunteers, expanded, induced to differentiate into SLCs, and cryopreserved until use. This procedure could be performed as often as required to store an adequate quantity of acellular nerves and cells independently from the urgency of patients. In this way, unlike cadaveric nerves cellularized with autologous or allogeneic SC or SLCs, when a patient presenting PNI needs to be grafted, the acellular scaffolds could be recellularized with SLCs and ready for use within a lapse of 48 h.

5. Conclusion

Having the above perspectives in mind, in this study, we showed here that SLCs (ovines) can grow in vitro on acellular xenogeneic (human) sciatic nerve scaffolds. The SLCs growing on the xenogeneic scaffold were functional. The xenogeneic scaffold recellularized with allogeneic SLCs can be implanted in an injured peripheral nerve, promoting their functional recovery, and at least after six months, the xenografts are not rejected.

Author contributions

F-E P-M contributed to planning this project, executed the laboratory experiments, collected analyzed the data, and contributed to writing the manuscript of this article and the artwork besides executing the statistical analysis. Y-A T-M. Contributed to executing this project and. M S-M contributed to the analyses of data, executing the artwork, and writing of this article. A S-D directed and contributed to the histology and cytochemistry analyses of grafts and NIC nerves and revised the manuscript's correspondent parts. M-M G-P participated in the electrophysiological analyses and made the surgery on ewes, S S-F contributed to planning this project, data analyses, and writing this article. R M-de-O-L, facilitated all the laboratory resources concerning histological and immunocytochemistry analyses. J-R G-F executed the electrophysiological analyses, H-G M-R conceived the original idea, facilitated all the laboratory infrastructure, prepared the grafts, directed the project, analyzed the data, contributed to writing the manuscript, and approved the final version of the manuscript. F V-C analyzed and approved the original idea, facilitated all the infrastructure and resources to obtain the cadaveric nerves, contributed to data analyses, and obtained the financial support for the project.

Declaration of competing interest

The authors declare that there are no conflicts of interest.

Acknowledgments

This research was awarded a grant from the National Council for Science and Technology (*Consejo Nacional de Ciencia y Tecnología*, CONACYT; Mexico, Grant PN 2017/6583). Florencia E Pedroza-Montoya was awarded a master's degree fellowship from CONACYT.

The authors thank Luis I. Botello-Soto, MD, for his technical assistance in processing the samples for morphological analysis and Tania S. Ortíz-Torres for her valuable collaboration in previous work on this project.

References

[1] Miclescu A, Straatmann A, Gkatziani P, Stephen Butler S, Rolf Karlsten R, Gordh T, et al. Chronic neuropathic pain after traumatic peripheral nerve injuries in the upper extremity: prevalence, demographic and surgical determinants, impact on health and on pain medication. Scand J Pain 2019;20:95–108.
[2] Naff NJ, Ecklund JM. History of peripheral nerve surgery techniques. Neurosurg Clin 2001;12:197–209.
[3] Kornfeld T, Vogt PM, Radtke C. Nerve grafting for peripheral nerve injuries with extended defect sizes. Wien Med Wochenschr 2018;169:240.
[4] Choi J, Kim JH, Jang JW, Kim HJ, Choi SH, Kwon SW. Decellularized sciatic nerve matrix as a biodegradable conduit for peripheral nerve regeneration. Neural Regen Res 2018;13:1796–803.
[5] Fernandez E, Signorelli F, Lucantoni C, D'Alessandris G, Lauretti L, Mariano Socolovsky M, et al. Peripheral nerve surgery: allo-grafts and conduits (alternatives to autografts?) in peripheral nerve regeneration. J Neurosurg 2006;105:602–9.
[6] Jahromi M, Razavi S, Bakhtiari A. The advances in nerve tissue engineering: from fabrication of nerve conduit to in vivo nerve regeneration assays. J Tissue Eng Regen Med 2019;13:2077–100.
[7] Klein S, Vykoukal J, Felthaus O, Thomas Dienstknecht T, Prantl L. Collagen type I conduits for the regeneration of nerve defects. Materials (Basel) 2016;9:219.
[8] Zhang PX, Han N, Kou Y-H, Qing-Tang Zhu Q-T, Xiao-Lin Liu X-L, Da-Ping Quan D-P, et al. Tissue engineering for the repair of peripheral nerve injury. Neural Regen Res 2019;14:51–8.
[9] Silva JB, Marchese JM, Cauduro CG, Debiasi M. Nerve conduits for treating peripheral nerve injuries: a systematic literature review. Hand Surg Rehabil 2017;36:71–85.
[10] Buckenmeyer MJ, Meder TJ, Prest TA, Brown BN. Decellularization techniques and their applications for the repair and regeneration of the nervous system. Methods 2020;171:41–61. 15.
[11] Wang D, Liu X-L, Zhu J-K, Hu J, Jiang L, Zhang Y, et al. Repairing large radial nerve defects by acellular nerve allografts seeded with autologous bone marrow stromal cells in a monkey model. J Neurotrauma 2010;27:1935–43.
[12] Wang D, Liu X-L, Zhu J-K, Jland L. Bridging small-gap peripheral nerve defects using acellular nerve allograft implanted with autologous bone marrow stromal cells in primates. Brain Res 2008;1188:44–53.
[13] Chernousov MA, Yu WM, Chen ZL, Carey DJ, Strickland S. Regulation of Schwann cell function by the extracellular matrix. Glia 2008;56:1498–507.
[14] Deumens R, Bozkurt A, Meek MF, Marcus MAE, Joosten EAJ, Weis J, et al. Repairing injured peripheral nerves: bridging the gap. Prog Neurobiol (Oxf) 2010;92:245–76.
[15] Zhang Y, Luo H, Zhang Z, Lu Y, Huang X, Yang L, et al. A nerve graft constructed with xenogeneic acellular nerve matrix and autologous adipose-derived mesenchymal stem cells. Biomaterials 2010;31:5312–24.
[16] Allodi I, Udina E, Navarro X. Specificity of peripheral nerve regeneration: interactions at the axon level. Prog Neurobiol (Oxf) 2012;98:16–37.
[17] Wang W, Itoh S, Takakuda K. Comparative study of the efficacy of decellularization treatment of allogeneic and xenogeneic nerves as nerve conduits. J Biomed Mater Res 2016;104:445–54.
[18] Radtke C, Allmeling C, Waldmann K-H, Kerstin Reimers K, Kerstin Thies K, Henning C, et al. Spider silk constructs enhance axonal regeneration and remyelination in long nerve defects in sheep. PLoS One 2011;6:e16990.
[19] Zhao Z, Wang Y, Peng J, Ren Z, Zhan S, Liu Y, et al. Repair of nerve defect with acellular nerve graft supplemented by bone marrow stromal cells in mice. Microsurgery 2011;31:388–94.
[20] García-Pérez MM, Martínez-Rodríguez HG, López-Guerra GG, Soto-Domínguez A, Said-Fernández SL, Morales-Avalos R, et al. A modified chemical protocol of decellularization of rat sciatic nerve and its recellularization with mesenchymal differentiated schwann-like cells: morphological and functional assessments. Histol Histopathol 2017;32:779–92.
[21] Wang X, Hu W, Cao Y, Yao J, Wu J, Gu X. Dog sciatic nerve regeneration across a 30-mm defect bridged by a chitosan/PGA artificial nerve graft. Brain 2005;128:1897–910.

[22] Soto-Domínguez A, Ballesteros-Elizondo RG, Santoyo-Pérez ME, Rodríguez-Rocha H, García-Garza R, Nava-Hernández MP, et al. Peroxisomicine A1 (toxin T-514) induces cell death of hepatocytes in vivo by triggering the intrinsic apoptotic pathway. Toxicon 2018;154:79–89.
[23] Jiang L, Zhu J-K, Liu X-L, Xiang P, Hu J, Yu W-H-. Differentiation of rat adipose tissue-derived stem cells into Schwann-like cells in vitro. Regen Transplant 2008;19:2015–9.
[24] Liu G, Cheng Y, Guo S, Feng Y, Li Q, Jia H, et al. Transplantation of adipose-derived stem cells for peripheral nerve repair. Int J Mol Med 2011;28:565–72.
[25] Wallis JM, Borg ZD, Daly AB, Deng B, Ballif BA, Allen GB, et al. Comparative assessment of detergent-based protocols for mouse lung de-cellularization and Re-cellularization. Tissue Eng C Methods 2012;18:420–32.
[26] Ide C, Tohyama K, Yokota R, Nitatori T, Onodera S. Schwann cell basal lamina and nerve regeneration. Brain Res 1983;288:61–75.
[27] Reglamento de la Ley General de Salud en Materia de Control Sanitario de la Disposición de Organos, Tejidos y Cadáveres de Seres Humanos (http://www.diputados.gob.mx/LeyesBiblio/regley/Reg_LGS_MCSOTCSH.pdf)
[28] Organ and tissue donation for transplantation – Organ and tissue donation (https://www.health.nsw.gov.au/organdonation/Pages/organ-tissue-donation-transplantation.aspx)
[29] Glazier A. Organ donation and the principles of gift law. Clin J Am Soc Nephrol 2018;13:1283–4. Published Online.
[30] Haastert-Talini K. Culture and proliferation of highly purified adult Schwann cells from rat, dog, and man. Methods Mol Biol 2012;846:189–200.
[31] Ray WZ, Susan E, Mackinnon SE. Management of nerve gaps: autografts, allografts, nerve transfers, and end-to-side neurorrhaphy. Exp Neurol 2010;223:77–85.
[32] Forden J, Xu QG, Khu KJ, Midha R. A long peripheral nerve autograft model in the sheep forelimb. Neurosurgery 2011;68:1354–62.
[33] Lawson GM, Glasby MA. Peripheral nerve reconstruction using freeze-thawed muscle grafts: a comparison with group fascicular nerve grafts in a large animal model. J R Coll Surg Edinb 1998;43:295–302.
[34] Casañas J, Torre J, Soler F, García F, Rodellar C, Pumarola M, et al. Peripheral nerve regeneration after experimental section in ovine radial and tibial nerves using synthetic nerve grafts, including expanded bone marrow mesenchymal cells: morphological and neurophysiological results. Injury 2014;45:S2–6.
[35] Gersey ZC, Burks SS, Anderson KD, Dididze M, Khan A, Dalton Dietrich WD, et al. First human experience with autologous Schwann cells to supplement sciatic nerve repair: report of 2 cases with long-term follow-up. Neurosurg Focus 2017;42:E2.
[36] Graham JB, Neubauer D, Xue Q-S, David Muir D. Chondroitinase applied to peripheral nerve repair averts retrograde Axonal regeneration. Exp Neurol 2007;203:185–95.
[37] Moore AM, MacEwan M, Santosa KB, Chenard KE, Ray WZ, Hunter DA, et al. Acellular nerve allografts in peripheral nerve regeneration: a comparative study. Muscle Nerve 2011;44:221–34.
[38] Safa B, Jain S, Desai MJ, Greenberg JA, Niacaris TR, Nydick JA, et al. Peripheral nerve repair throughout the body with processed nerve allografts: results from a large multicenter study. Microsurgery 2020;40:527–37.
[39] Wang Y, Tong XJ, Liu GB, Li Q, Zhang LX, Sun XH. Sciatic nerve repair by acellular nerve xenografts implanted with BMSCs in rats xenograft combined with BMSCs. Synapse 2012;66:256–69.
[40] Pover CM, Lisney SJ. Influence of autograft size on peripheral nerve regeneration in cats. J Neurol Sci 1989;90:179–85.
[41] Karabekmez FE, Duymaz A, Moran SL. Early clinical outcomes with the use of decellularized nerve allograft for repair of sensory defects within the hand. Hand 2009;4:245–9.